Journal of Sound and Vibration (2002) **251**(3), 519–542
doi:10.1006/jsvi.2001.3995, available online at http://www.idealibrary.com on IDEAL®

CHAOS, CHAOS CONTROL AND SYNCHRONIZATION OF A GYROSTAT SYSTEM

Z.-M. Ge and T.-N. Lin

Department of Mechanical Engineering, National Chiao Tung University, 1001 *Ta Hsueh Road, Hsinchu* 30050, *Taiwan, Republic of China. E-mail*: *zmg@cc.nctu.edu.tw*

(*Received* 21 *May* 2001, *and in final form* 24 *September* 2001)

The dynamic behavior of a gyrostat system subjected to external disturbance is studied in this paper. By applying numerical results, phase diagrams, power spectrum, period-T maps, and Lyapunov exponents are presented to observe periodic and choatic motions. The effect of the parameters changed in the system can be found in the bifurcation and parametric diagrams. For global analysis, the basins of attraction of each attractor of the system are located by employing the modified interpolated cell mapping (MICM) method. Several methods, the delayed feedback control, the addition of constant torque, the addition of periodic force, the addition of periodic impulse torque, injection of dither signal control, adaptive control algorithm (ACA) control and bang–bang control are used to control chaos effectively. Finally, synchronization of chaos in the gyrostat system is studied.

© 2002 Elsevier Science Ltd.

1. INTRODUCTION

In the past one-and-half decades, a large number of studies have shown that chaotic phenomena are observed in many physical systems that possess non-linearity [1, 2]. It was also reported that the chaotic motion occurred in many non-linear control systems [3, 4]. Many studies of the satellite have been accomplished in recent years [5, 6]. It is possible to reorient a torque-free satellite by transferring angular momentum between the satellite and internal rotors using internal torques. If the rotors are axisymmetric and constrained to relative rotation about their symmetric axes, then the system is called a gyrostat [7–9]. In this paper, there are three rotors which are orthogonalized to each other in the gyrostat. One of the angular momentums of rotors is distributed by a sinusoidal ripple. The non-linear dynamics, chaotic control and synchronization of this gyrostat system will be studied in this paper.

A lot of modern techniques are used in analyzing the deterministic non-linear gyrostat system behavior. Computational methods are employed to obtain the characteristics of the non-linear gyrostat system. By applying numerical results, phase diagrams, power spectrum, period-T maps, and Lyapunov exponents are presented to observe periodic and chaotic motions. The effect of the parameters changed in the system can be found in the bifurcation and parametric diagrams. For global analysis, the basins of attraction of each attractors of the system are located by employing the modified interpolated cell mapping (MICM) method. Attention is shifted to the controlling chaos. For this purpose, the delayed feedback control, the addition of constant torque, the addition of periodic force, the addition of periodic impulse torque, injection of dither signal control, adaptive control algorithm (ACA) control and bang–bang control are used to control chaos. Finally, synchronization [10] of chaos in the gyrostat system is studied.

0022-460X/02/130519 + 24 $35.00/0 © 2002 Elsevier Science Ltd.

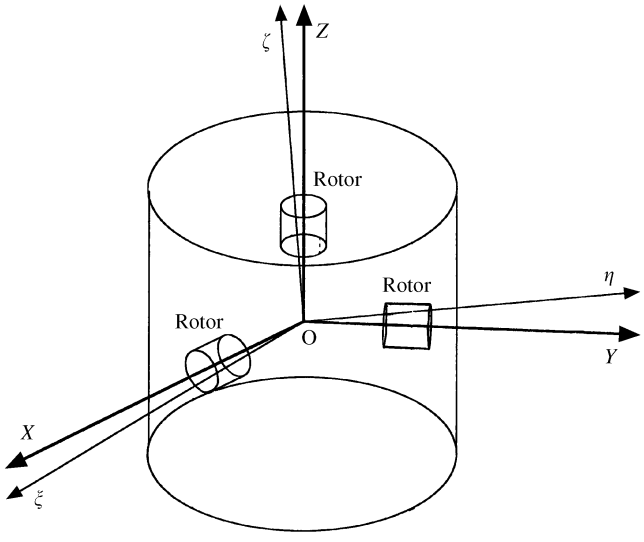

Figure 1. System model.

2. EQUATIONS OF MOTION

The system considered here is depicted in Figure 1. Assume that there are three rotors in a satellite. Let $O\xi\eta\zeta$ be an inertia orthogonal co-ordinate system with origin at mass center O of satellite. Let $OXYZ$ be a rotating orthogonal co-ordinate system with satellite and OX, OY and OZ be the three principal axes of inertia, respectively, ω_x, ω_y, ω_z are the projections of the angular velocity on X-, Y-, Z-axis respectively. A, B, C are the principal moments of inertia. The angular moments of rotors h_1, h_2, h_3 are located at OX, OY, OZ. The angular moment of rotor h_3 is represented by a constant and harmonic term $h_3(1 + f\cos\omega t)$, where h_3, f, ω are constants. ω_r is the projection of the angular velocity of satellite on X-, Y-, Z-axis which is designed. Add the feedback terms to control the angular velocity ω_x, ω_y, ω_z to ω_r. Let $\omega_x = x$, $\omega_y = y$, $\omega_z = z$, the equation of motion can be expressed as

$$\dot{x} = \frac{(B-C)}{A}yz - \frac{h_3}{A}(1 + f\cos\omega t)y + \frac{h_2}{A}z + \frac{k_1}{A}(\omega_r - x) + \frac{k_2}{A}(\omega_r^2 - x^3),$$

$$\dot{y} = \frac{(C-A)}{B}xz - \frac{h_1}{B}z + \frac{h_3}{B}(1 + f\cos\omega t)x + \frac{k_3}{B}(\omega_r - y) + \frac{k_4}{B}(\omega_r^3 - y^3),$$

$$\dot{z} = \frac{(A-B)}{C}xy + \frac{h_3}{C}f\omega\sin\omega t - \frac{h_2}{C}x + \frac{h_1}{C}y - \frac{b}{C}z + \frac{k_5}{C}(\omega_r - z) + \frac{k_6}{C}(\omega_r^3 - z^3), \quad (1)$$

where equation (1) contained non-linear feedback terms, and b is the damping coefficient. $A = 500$, $B = 500$, $C = 1000$, $h_1 = h_2 = 200$, $h_3 = 250$, $b = 200$, $\omega = 1.0$, k_i $(i = 1, \ldots, 6) = 1$, $\omega_r = 0$.

3. PHASE PORTRAITS, PERIOD-T MAP AND POWER SPECTRUM

The phase plane is the evolution of a set of trajectories emanating from various initial conditions in the state space. When the solution reaches a stable state, the asymptotic

behavior of the phase trajectories is of particular interest and the transient behavior in the system is neglected. The period-T map, where T is the time period of the forcing, is a better

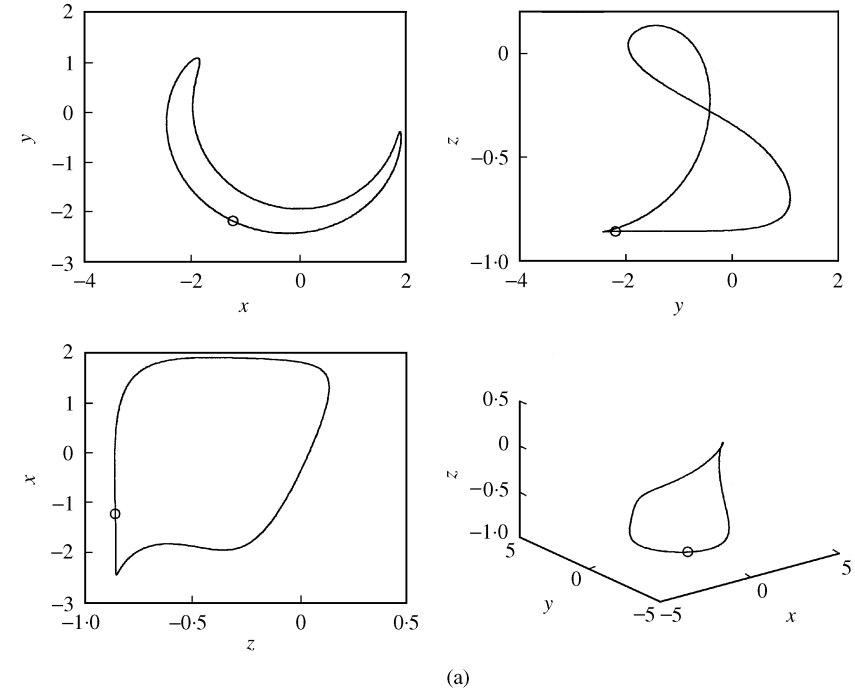

(a)

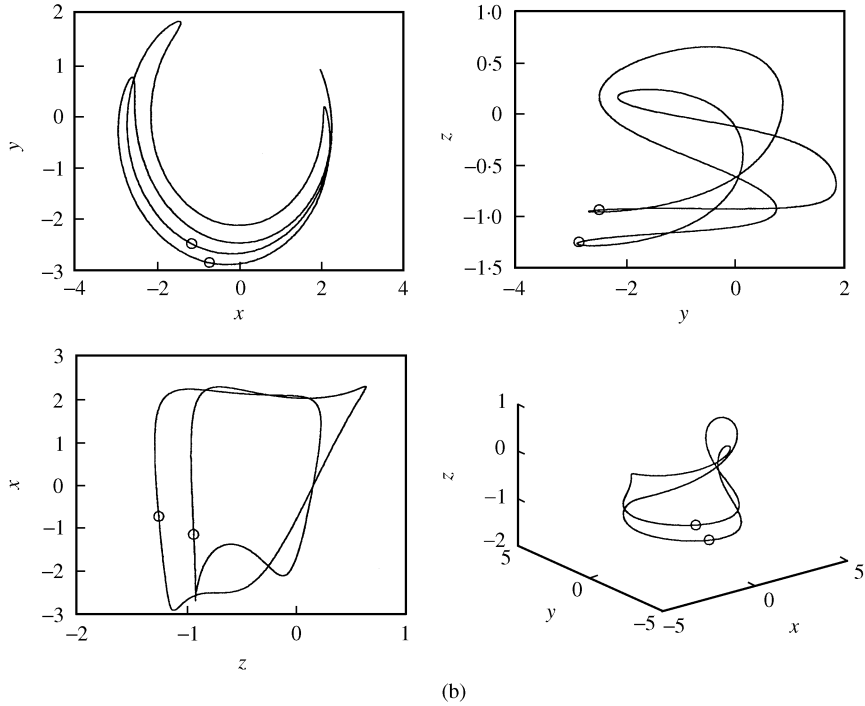

(b)

Figure 2. (a) Phase portrait and period-1T map "$\circ$" for $f = 4{\cdot}5$. (b) Phase portrait and period-2T map "$\circ$" for $f = 5{\cdot}5$. (c) Phase portrait and period-4T map "$\circ$" for $f = 6{\cdot}15$. (d) $f = 6{\cdot}5$, phase portraits and period-T map "$\cdot$" of chaos.

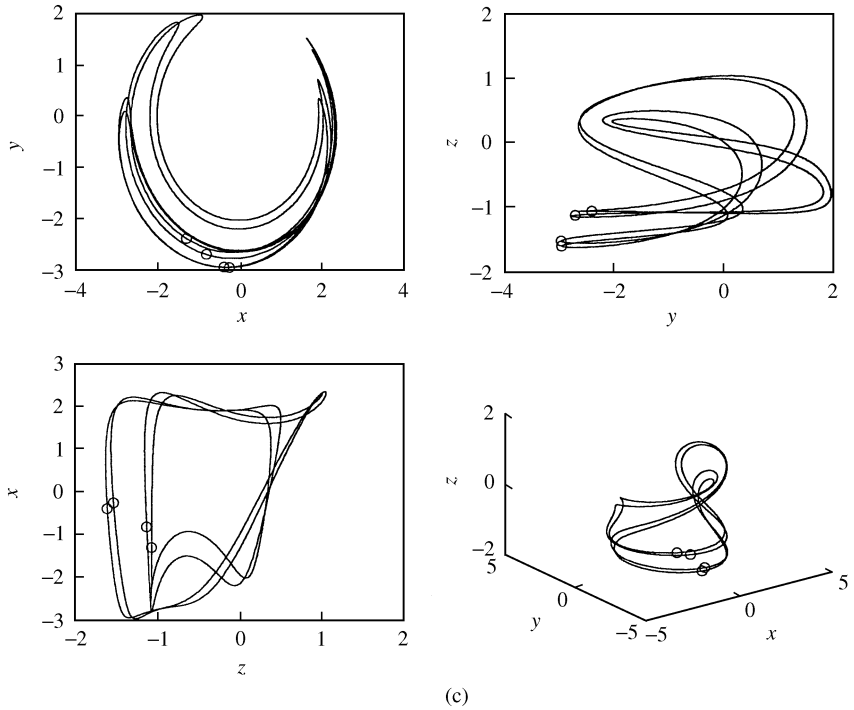

Figure 2. Continued.

method for displaying the dynamics. Equation (1) is plotted in Figure 2(a–c) for $f = 4{\cdot}5$, $5{\cdot}6$ and $6{\cdot}15$ respectively. Clearly, the motion is periodic. But Figure 2(d), for $f = 6{\cdot}5$ shows the chaotic state. The points of the period-T map become irregular.

Another technique for the identification and characterization of the system is power spectrum. It is often used to distinguish between periodic, quasi-periodic and chaotic behavior for a dynamical system. Any function $x(t)$ may be represented as a superposition of different periodic components. The determination of their relative strength is called spectral analysis. If it is periodic, the spectrum may be a linear combination of oscillations whose frequencies are integer multiples of basic frequency. The linear combination is called a Fourier series. If it is not periodic, the spectrum must then be in terms of oscillations with a continuum of frequencies. Such a representation of the spectrum is called Fourier integral of $x(t)$. The representation is useful for dynamical analysis. The non-autonomous systems are observed by the portraits of power spectrum in Figure 3(a–c) for period-1T period-2T and period-4T steady state vibration. As $f = 6{\cdot}5$ chaos occurs; the spectrum is a broad band and the peak is still present at the fundamental frequency shown in Figure 3(d). The noise-like spectrum is the characteristic of a chaotic dynamical system.

4. BIFURCATION DIAGRAM AND PARAMETER DIAGRAM

In the previous section, the information about the dynamics of the non-linear system for specific values of the parameters is provided. The dynamics may be viewed more completely over a range of parameter values. As the parameter is changed, the equilibrium points and periodic motions can be created or destroyed, or their stability can be lost. The

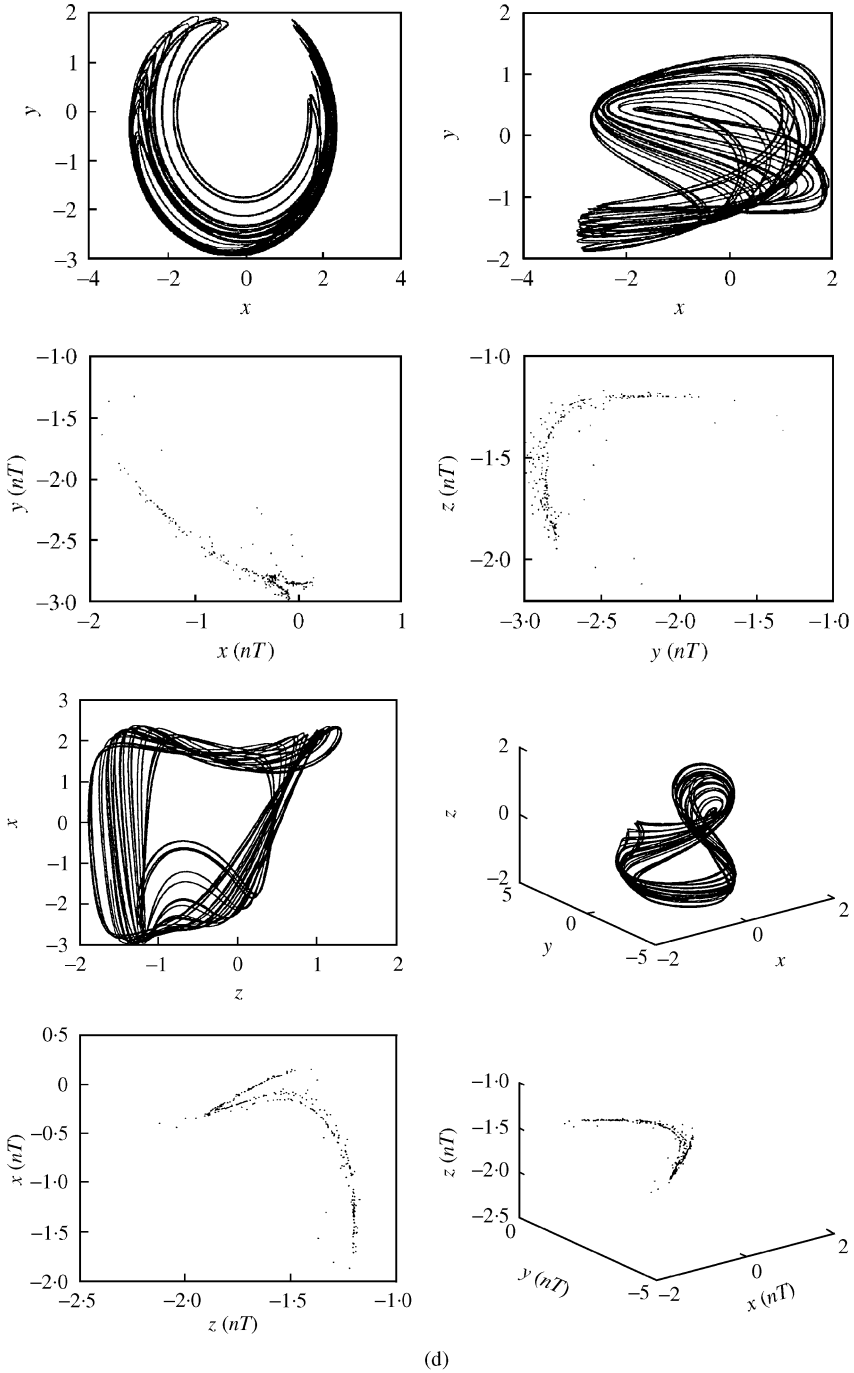

(d)

Figure 2. Continued.

phenomenon of sudden change in the motion as a parameter is varied is called bifurcation, and the parameter values at which they occur are called bifurcation points. The bifurcation diagram of the non-linear system of equations is depicted in Figure 4. $f \in [4{\cdot}5, 6{\cdot}5]$ with the incremental value of f is 0·01.

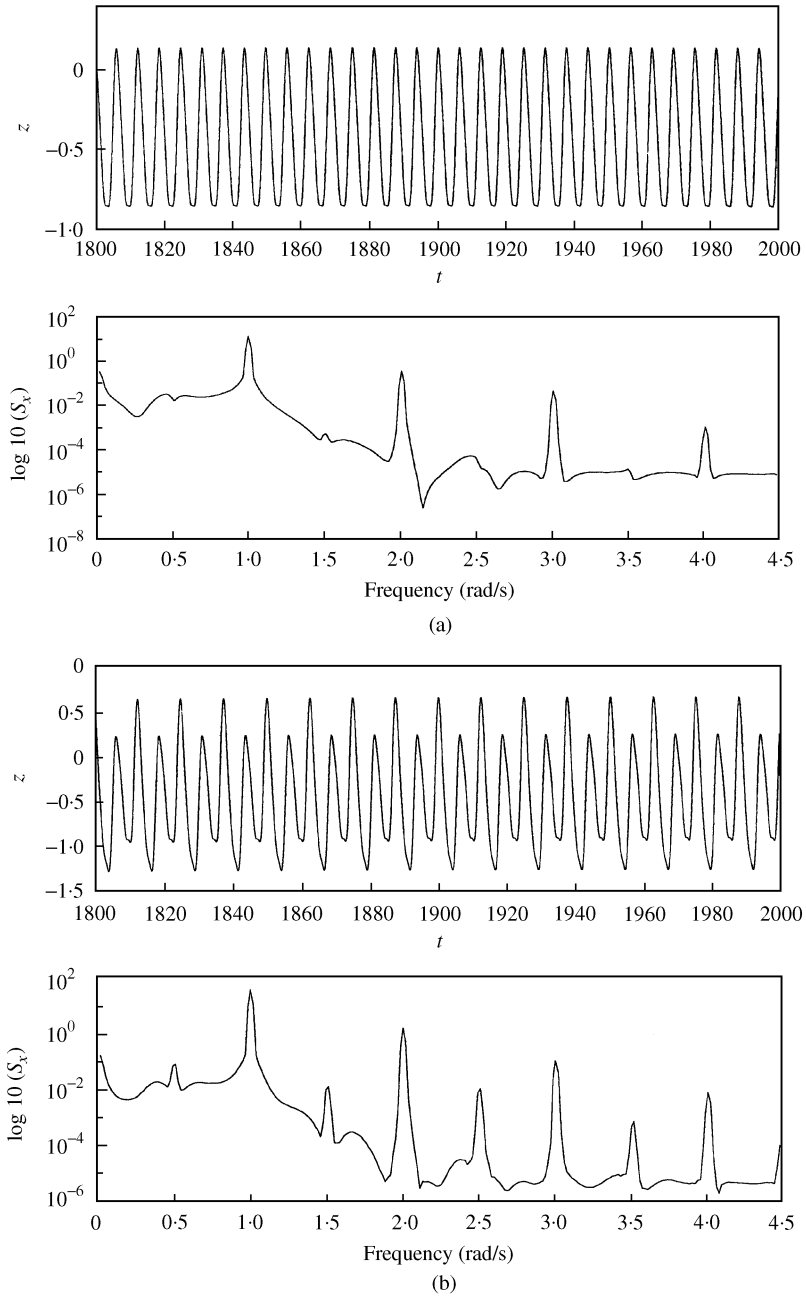

Figure 3. (a) Power spectrum and time history of period-1T for $f = 4{\cdot}5$. (b) Power spectrum and time history of period-2T for $f = 5{\cdot}5$. (c) Power spectrum and time history of period-4T for $f = 6{\cdot}15$. (d) Power spectrum and time history of chaos for $f = 6{\cdot}5$.

Further, the parameter value f and k_i $(i = 1, \ldots, 6)$ will also be varied to observe the behaviors of bifurcation of the system. The parameter diagrams are shown in Figure 5.

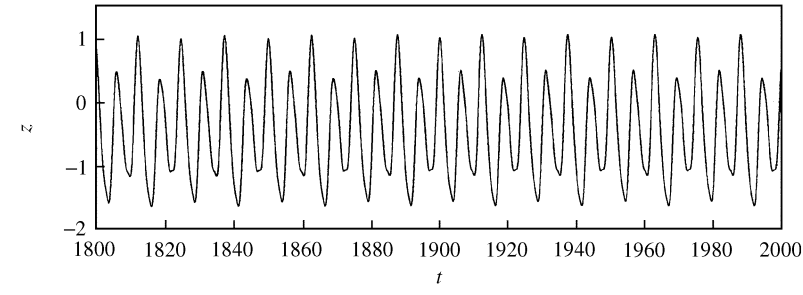

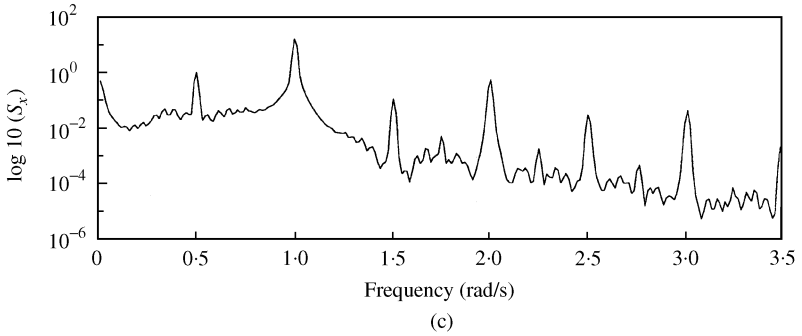

(c)

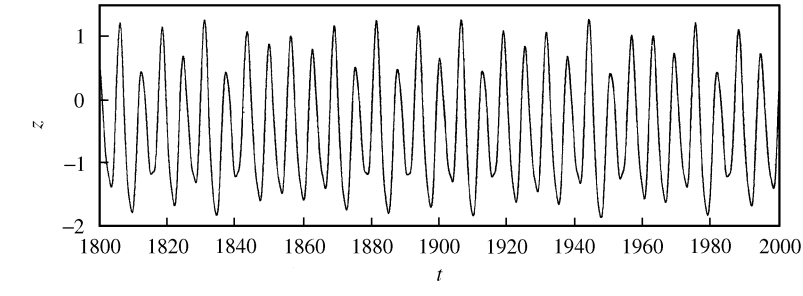

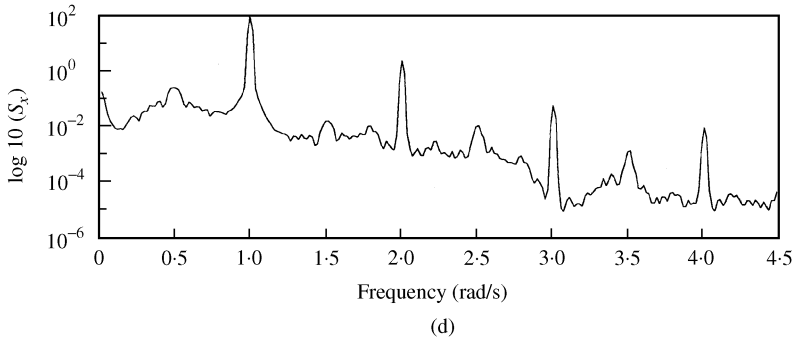

(d)

Figure 3. Continued.

5. LYAPUNOV EXPONENT AND LYAPUNOV DIMENSION

The Lyapunov exponent may be used to measure the sensitive dependence upon initial conditions. It is an index for chaotic behavior. Different solutions of a dynamic system, such as fixed points, periodic motions, quasi-periodic motion, and chaotic motion can be

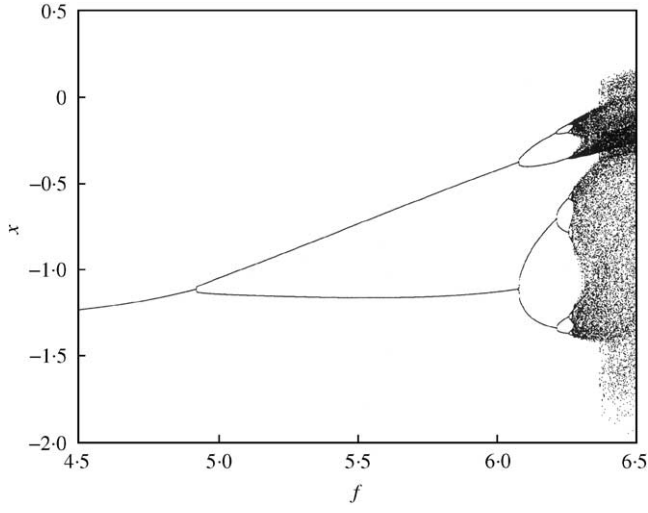

Figure 4. Bifurcation diagram of f versus x.

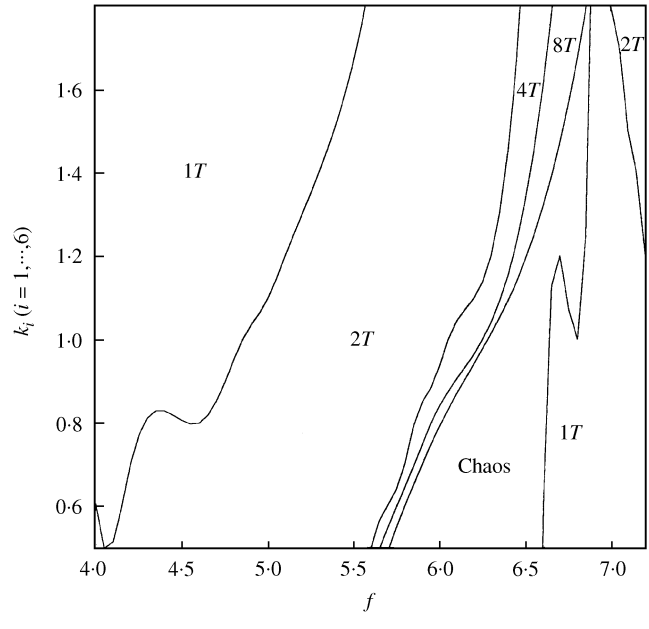

Figure 5. Parameter diagram of f versus k_i $(i = 1, \ldots, 6)$.

distinguished by it. If two trajectories start close to one another in phase space, they will move exponentially away from each other for small times on the average. Thus, if d_0 is a measure of the initial distance between the two starting points, the distance is $d(t) = d_0 2^{\lambda t}$. The symbol λ is called the Lyapunov exponent. The divergence of chaotic orbits can only be locally exponential, because if the system is bounded, $d(t)$ cannot grow to infinity. A measure of this divergence of orbits is such that the exponential grown at many points along a trajectory has to be averaged. When $d(t)$ is too large, a new "nearby" trajectory $d_0(t)$ is

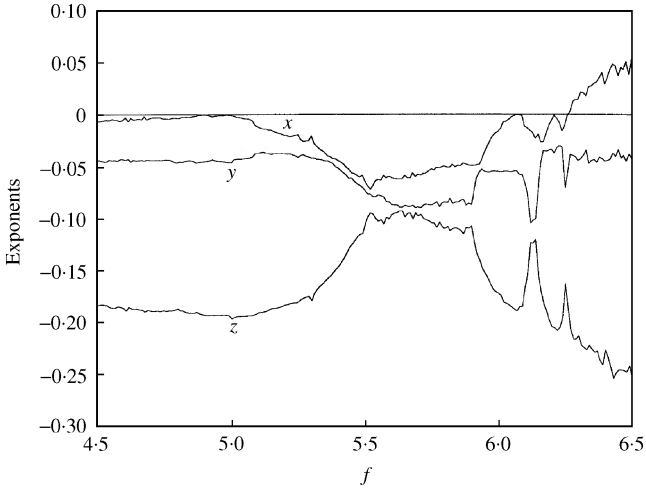

Figure 6. The Lyapunov exponents for f between 4·5 and 6·5.

TABLE 1

Lyapunov exponents and Lyapunov dimensions of the system for different f

f	λ_1	λ_2	λ_3	λ_4	$\sum \lambda_i$	d_L	
4·5	– 0·0053	0	– 0·0441	– 0·1839	– 0·242	1	Period-1
5·5	– 0·0643	0	– 0·0733	– 0·1047	– 0·242	1	Period-2
6·16	– 0·0183	0	– 0·0682	– 0·1561	– 0·242	1	Period-4
6·5	0·0445	0	– 0·0519	– 0·2343	– 0·242	2·85	Chaos

defined. The Lyapunov exponent can be expressed as

$$\lambda = \frac{1}{t_N - t_0} \sum_{k=1}^{N} \log_2 \frac{d(t_k)}{d_0(t_{k-1})}. \tag{2}$$

The signs of the Lyapunov exponents provide a qualitative picture of a system dynamics. The criteria are

$$\lambda > 0 \quad \text{(chaotic)}, \qquad \lambda \leqslant 0 \quad \text{(regular motion)}.$$

The periodic and chaotic motions can be distinguished by the bifurcation diagram, while the quasi-periodic motion and chaotic motion may be confused. However, they can be distinguished by the Lyapunov exponent method. The Lyapunov exponents of the solutions of the non-linear dynamic system are plotted in Figure 6 as $f = 4{\cdot}5$–$6{\cdot}5$.

There are a number of different fractional-dimension-like indices, e.g., the information dimension, Lyapunov dimension, and correlation exponent, etc., the difference between them is often small. The Lyapunov dimension is a measure of the complexity of the attractor. It has been developed [11] such that the Lyapunov dimension d_L is introduced as

$$d_L = j + \frac{\sum_{i=1}^{j} \lambda_i}{|\lambda_{j+1}|}, \tag{3}$$

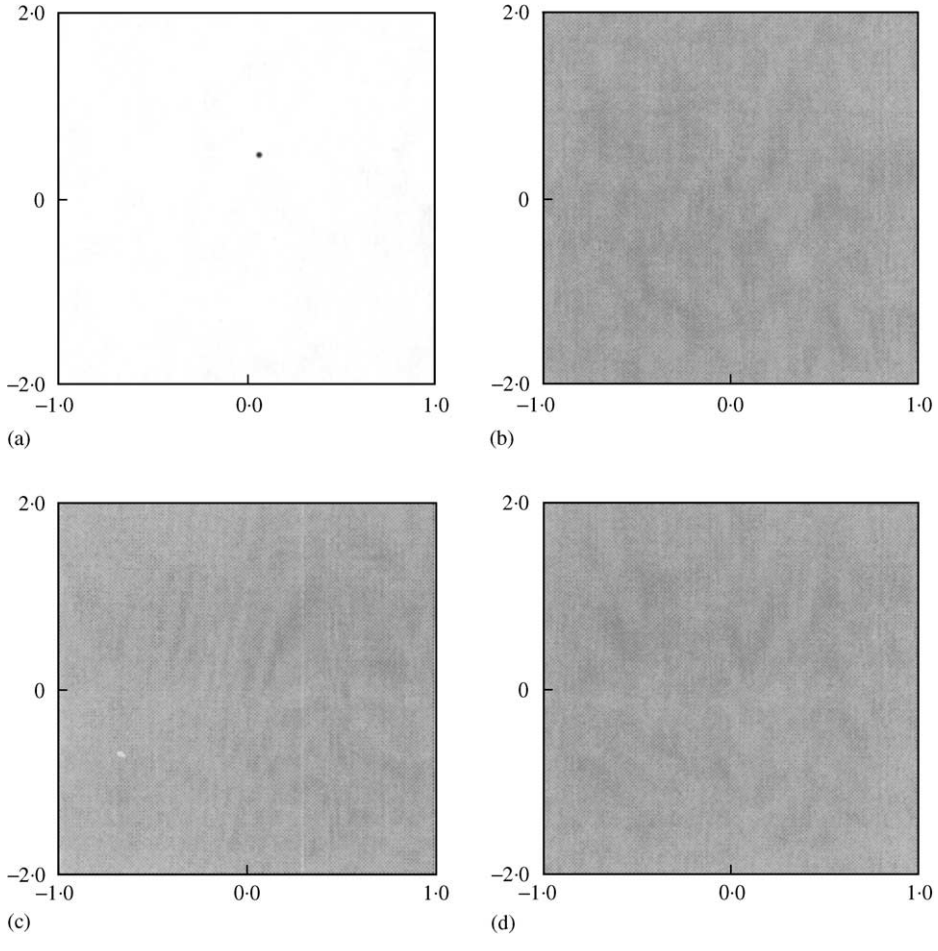

Figure 7. (a) The projection of attractors; (b) Basins of attraction for $z = -3$; (c) $z = 0$; (d) $z = 3$ for $f = 4{\cdot}5$.

where j is defined by the condition

$$\sum_{i=1}^{j} \lambda_i > 0 \quad \text{and} \quad \sum_{i=1}^{j+1} \lambda_i < 0.$$

The Lyapunov dimension for a strange attractor is a non-integer number. The Lyapunov dimension and the Lyapunov exponent of the non-linear system are listed in Table 1 for different values of f.

6. GLOBAL ANALYSIS BY MODIFIED INTERPOLATED CELL MAPPING METHOD

A brief introduction of the modified interpolated mapping method [12] is given as follows. Consider that a point mapping system is governed by

$$X_{n+1} = f(X_n), \quad X \in R^3, \tag{4}$$

where $f: R^3 \to R^3$ and n is an integer. The basic concept of the interpolated mapping method is to find the image X_{n+1} by using an interpolation procedure instead of the system. For

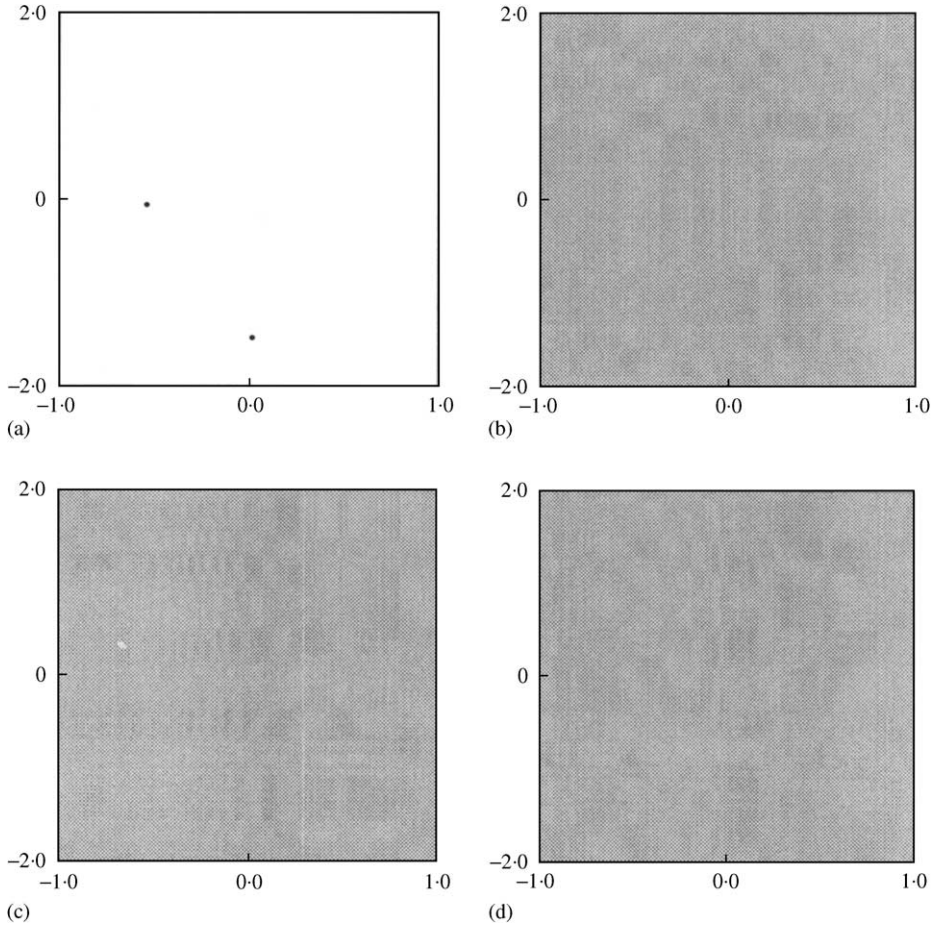

Figure 8. (a) The projection of attractors; (b) Basins of attraction for $z = -3$; (c) $z = 0$; (d) $z = 3$ for $f = 5{\cdot}5$.

a three-dimensional system, the interested region D is specified by a Cartesian product $[x_{1\,min}, x_{1\,max}] \times [x_{2\,min}, x_{2\,max}] \times [x_{3\,min}, x_{3\,max}]$, which is divided into $N_1 \times N_2 \times N_3$ cells. The size of a cell is $S_i = (x_{i\,max} - x_{i\,min})/N_i$, $i = 1, 2, 3$. The first mappings of cells in the region of interest are constructed by numerical integration to serve as the reference mappings for the interpolation. The interpolated mappings of each cell are constructed within the mapping periods assigned, such as 30 periods. Through these mapping sequences, periodic attractors with periods of less than 30 are located by the 10^{-5} cell size criterion. If no periodic attractor is located, the 30th mapping of each cell is assigned to the first mapping, and then iterated forward to construct the next iteration of 30 mappings. If periodic attractors are located and a cell leads to a periodic attractor within the 10^{-2} cell size criterion, the cell is considered in the basin of attraction of the attractor.

For a three-dimensional system, 303^3 cells are studied by the modified interpolated mapping method, where 303 is the number of the total cells divided in each dimensional of the region of interest.

Figure 7(a) for $f = 4{\cdot}5$ indicates that the system motion is period-1T motion and the corresponding basins of attraction is shown in Figure 7(b–d) with $z = -1{\cdot}0$, 0, $1{\cdot}0$ respectively. For $f = 5{\cdot}5$, Figure 8(a–d) shows the phenomena of period-2T motion. Only one symbol "." is presented, which shows that the system has only an attractor.

7. CONTROLLING CHAOS

Several kinds of interesting non-linear dynamic behaviors of the system have been studied in previous sections. They have shown that the forced system exhibited both regular and chaotic motions. Usually, chaos is unwanted or undesirable.

In order to improve the performance of a dynamic system or avoid the chaotic phenomena, we need to control a chaotic system to a periodic motion which is beneficial for working with a particular condition. It is thus of great practical importance to develop suitable control methods. Very recently, much interest has been focused on this type of problem—controlling chaos [13–17]. For this purpose, the delayed feedback control, the addition of constant torque, the addition of periodic force, the addition of periodic impulse torque, injection of dither signal control, adaptive control algorithm (ACA) control and bang–bang control are used to control chaos. As a result, the chaotic system can be controlled.

7.1. CONTROLLING OF CHAOS BY DELAYED FEEDBACK CONTROL

Let us consider a dynamic system which can be simulated by ordinary differential equations. We imagine that the equations are unknown, but some scalar variables can be measured as a system output. The idea of this method is that the difference $D(t)$ between the delayed output signal $y(t-\tau)$ and the output signal $y(t)$ is used as a control signal. In other words, we used a perturbation of the form

$$F(t) = K_A[y(t-\tau) - y(t)] = KD(t). \tag{5}$$

Here τ is the delay time. Choose an appropriate weight K_A and τ of the feedback and one can achieve the periodic state. If $K_A = 0{\cdot}2$, and $\tau = 1$, the results are shown in Figure 9.

This control is achieved by the use of the output signal, which is fed back into the system. The difference between the delayed output signal and the output signal itself is used as a control signal. Only a simple delay line is required for this feedback control. To achieve the periodic motion of the system, two parameters, namely, the time of delay τ and the weight K_A of the feedback, should be adjusted.

7.2. CONTROLLING OF CHAOS BY ADDITION OF CONSTANT TORQUE

Interestingly, one can even add just a constant term to control or quench the chaotic attractor to a desired periodic one in a typical non-linear non-autonomous system. It

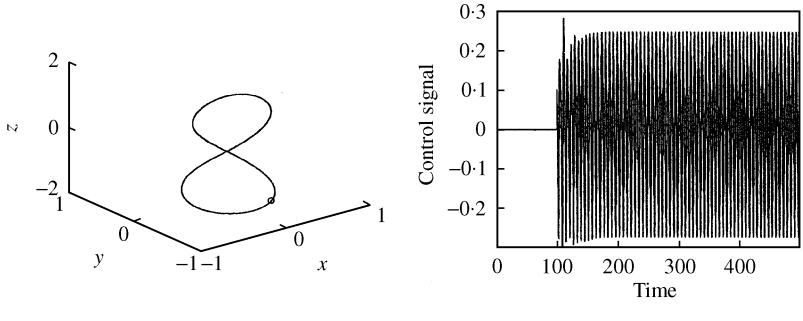

Figure 9. $K_A = 0{\cdot}2$, the period-1T motion of system after feedback control.

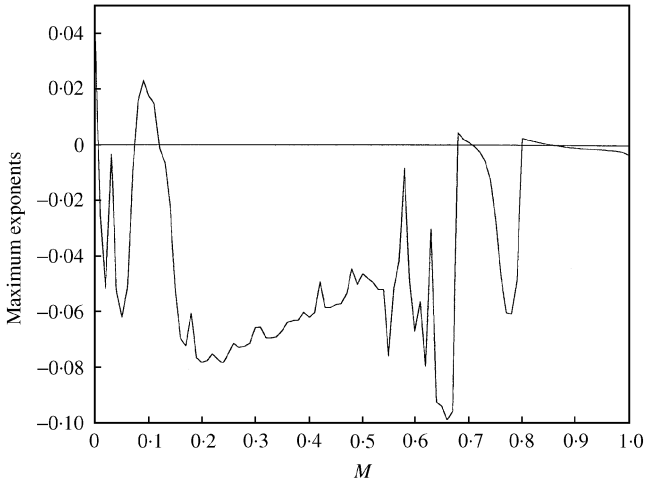

Figure 10. The maximal Lyapunov exponents against M.

ensures effective control in a very simple way. In order to understand this simple controlling approach in a better way, this method is applied to system (1) numerically.

In the absence of the constant motor torque, the system exhibits chaotic behavior under the parameter condition $f = 6{\cdot}5$.

Consider the effect of the constant motor torque M added to the right-hand side of the last equation of equation (1). By increasing its value from zero upwards, the chaotic behavior is altered. Spectral analysis of the Lyapunov exponents has proven to be the most useful dynamical diagnostic tool for examining chaotic motions. In Figure 10, the maximal Lyapunov exponents are shown. It is clear that the system returns to regular motion, when the constant torque M is presented at a certain interval.

7.3. CONTROL OF CHAOS BY ADDITION OF PERIODIC FORCE

One can control system dynamics by the addition of external periodic force in the chaotic state. For our purpose, the added periodic force, $N\sin(\bar{\omega}t + \phi)$, added to the right-hand side of the last equation of equation (1), is given. The system can then be investigated by a numerical solution, with the remaining parameter fixed. One case to examine the change in the dynamics of the system as a function of N for fixed $\bar{\omega} = \pi/4$, $\phi = 0$ and $\bar{\omega}$ for fixed $N = 1$, $\phi = 0$. The maximal Lyapunov exponents are estimated numerically; the results are shown in Figure 11(a) and 11(b) respectively. At certain intervals, the maximal Lyapunov exponents $\lambda_i \leqslant 0$, which indicates that the predictability of the system recovers.

7.4. CONTROLLING CHAOS BY ADAPTIVE CONTROL ALGORITHM (ACA)

Recently, Huberman and Lumer [16] have suggested a simple and effective adaptive control algorithm which utilizes an error signal proportional to the difference between the goal output and actual output of the system. The error signal governs the change of parameters of the system, which readjusts so as to reduce the error to zero. This method can be explained briefly: the system motion is set back to a desired state X_s by adding dynamics

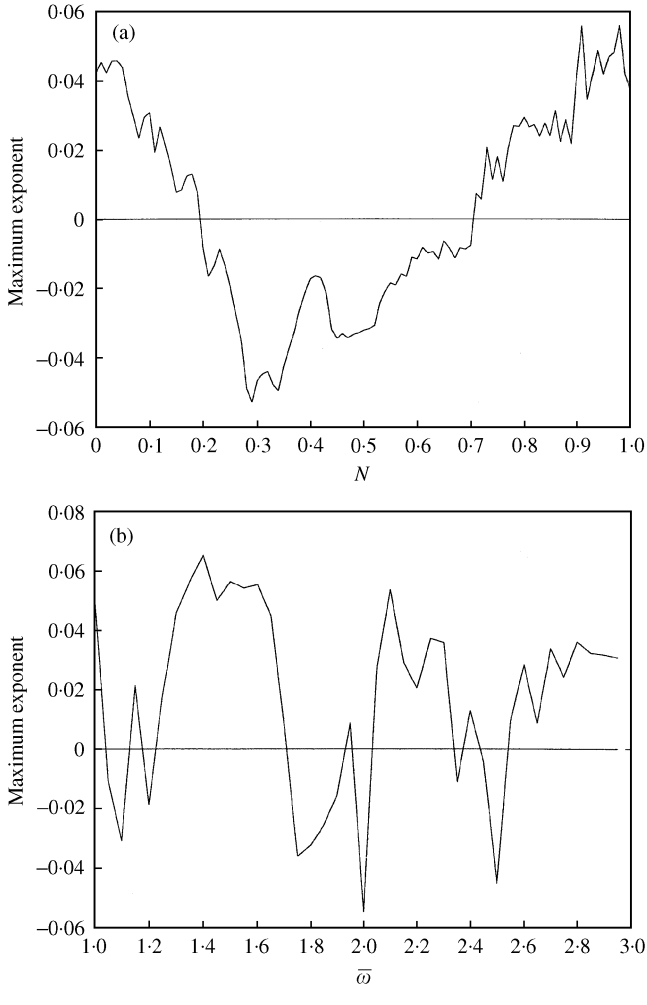

Figure 11. The maximal Lyapunov exponents against (a) N with $\bar{\omega} = \pi/4$, $\phi = 0$; (b) $\bar{\omega}$ with $N = 1$, $\phi = 0$.

to the control parameter P through the evolution equation

$$P = K_D G(X - X_s), \tag{6}$$

where the function G is proportional to the difference between X_s and the actual output X, and K_D indicates the stiffness of the control. The function G could be either linear or non-linear. In order to convert the dynamics of system (1) from chaotic motion to the desired periodic motion X_s, the chosen parameter A is perturbed as

$$\dot{A} = K_D(X - X_s). \tag{7}$$

If $K_D = 1$, the system can reach the period-1T, period-2T, as shown in Figure 12(a) and 12(b).

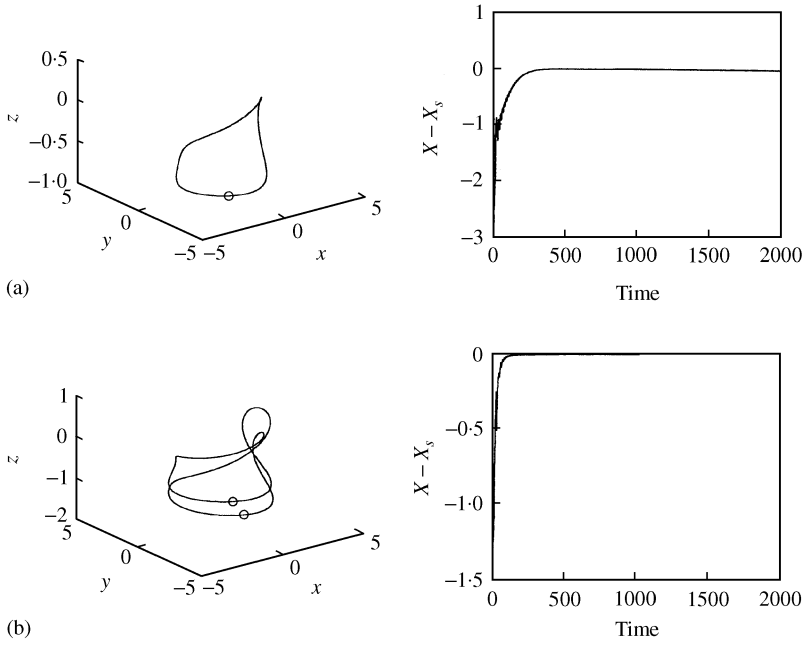

Figure 12. (a) The period-1T and (b) period-2T motion of system after Adaptive control.

7.5. CONTROLLING CHAOS BY BANG–BANG CONTROL

Time delay map is used in this control algorithm. Let error

$$e(t) = z(t) - z(t - \tau), \tag{8}$$

where τ is the external torque frequency. Define $V(t) = e(t)^2$ which is always positive or zero:

$$\dot{V} = 2e(t)\dot{e}(t) \tag{9}$$

if $\dot{V} \leqslant 0$ then $V(t) \to 0$; $e(t) \to 0$ and $z(t) \to z(t - \tau)$.

By detecting as to whether equation (9) is less than or greater than zero, the control law can be determined. Assume

$$\dot{x} = F_1(x, y, z, t), \qquad \dot{y} = F_2(x, y, z, t), \qquad \dot{z} = F_3(x, y, z, t) + u. \tag{10}$$

If $\| e(t) \| \leqslant \delta$, where $\delta > 0$ is a preset small value, $u(t) = 0$. If $\| e(t) \| > \delta$ then

$$u(t) = \begin{cases} -K_E(F_3(x, y, z, t) - \dot{z}(t - \tau)) & \text{when } e(t) > 0, \\ K_E(F_3(x, y, z, t) - \dot{z}(t - \tau)) & \text{when } e(t) < 0. \end{cases}$$

These results are similar to those in the case of an external force control and delayed feedback control. However, external perturbation or computation is needed for this control. If $K_E = 0{\cdot}07$, the system can reach the period-4T as shown in Figure 13.

7.6. CONTROLLING CHAOS BY ADDITION OF PERIODIC IMPULSE

Instead of perturbing system parameters, a technique for suppressing chaos is the application of a period impulse input to the system. Assume that the system is controlled by

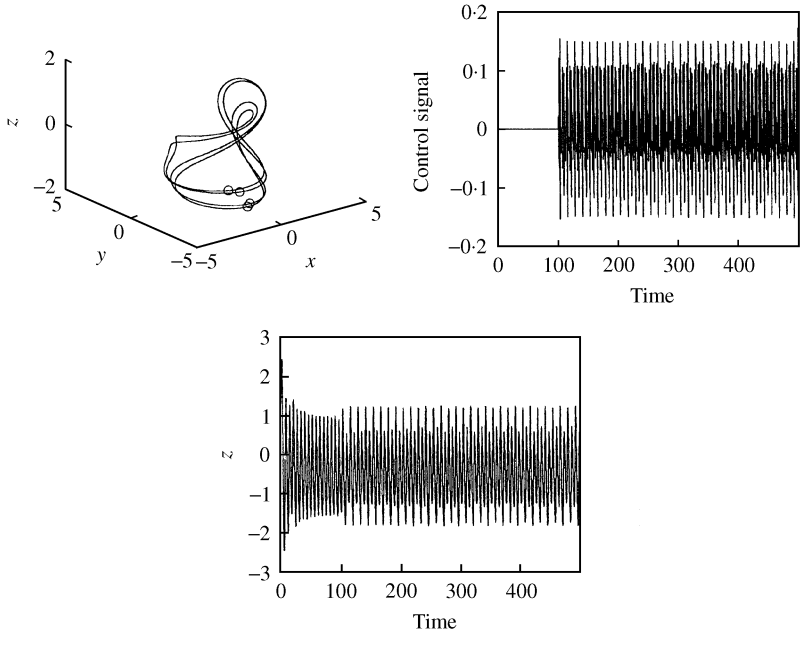

Figure 13. Bang–bang control which is used to control period-4T for $K_E = 0{\cdot}07$.

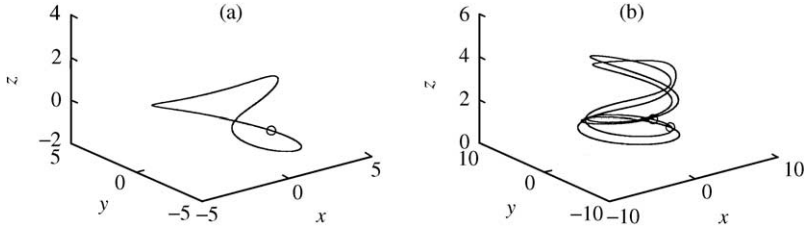

Figure 14. (a) The period-1T motion of system after period impulse control for $K_F = 0{\cdot}4$. (b) The period-2T motion of system after period impulse control for $K_F = 0{\cdot}6$.

a periodic impulse input F^*, where

$$F^* = K_F \sum_{j=0}^{\infty} \delta(t - jk_p),$$

K_F is a constant impulse intensity, k_p is the period between two consecutive impulses, and δ is the standard Kronecker delta function.

With different values of K_F and k_p, the controlled system can be stabilized at different periodic solutions. For example, when we fix the parameter $k_p = 0{\cdot}01$ and adjust impulse intensity K_F, the chaotic behavior disappears. For $K_F = 0{\cdot}4$ and $0{\cdot}6$, the system can reach the period-1T and period-2T as shown in Figure 14(a) and 14(b) respectively.

7.7. CONTROLLING CHAOS BY INJECTING DITHER SIGNAL CONTROL

In this section, we show that injection of another external input, called a dither signal which only adjusts the non-linear terms, into this chaotic system, can control the chaotic

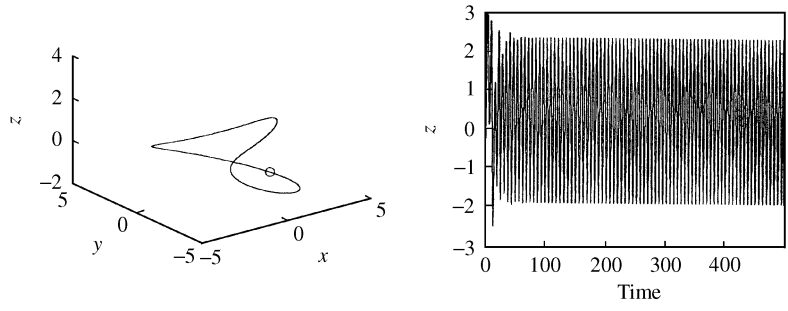

Figure 15. The period-1T motion of system after injecting dither signal control.

behavior. Using the dither signal method, on the system input, one can convert a chaotic motion on the system input to a periodic orbit or a steady motion. This approach is different from the weak periodic perturbation method, in which the external periodic torque must be coupled to a control parameter and its amplitude or frequency usually needs trial and error. First, define a square-wave dither signal

$$\mu = \tfrac{1}{2}\,[\,f(x + w) + f(x - w)], \tag{11}$$

then inject the dither signal into the system. The system equation is formed as follows:

$$\dot{x} = \tfrac{1}{2}\,[\,f_1(x + w, y + w, z + w, \tau) + f_1(x - w, y - w, z - w, \tau)], \tag{12}$$

$$\dot{y} = \tfrac{1}{2}\,[\,f_2(x + w, y + w, z + w, \tau) + f_2(x - w, y - w, z - w, \tau)], \tag{13}$$

$$\dot{x}_3 = \tfrac{1}{2}\,[\,f_3(x + w, y + w, z + w, \tau) + f_3(x - w, y - w, z - w, \tau)]. \tag{14}$$

For equation (14), whose frequency and amplitude are 100 and 0·7, the system is controlled to period-1T as shown in Figure 15.

8. SYNCHRONIZATION OF CHAOS

The concept of chaos synchronization emerged much later—not until the gradual realization of the usefulness of chaos by scientists and engineers. Chaotic signals are usually broad band and noise-like. Because of this property, synchronized chaotic systems can be used as cipher generators for secure communication. Several methods of synchronization have been studied in many theoretical model equations and electrical systems [18–21], recently. In this section, chaos synchronization for the mechanical system—gyrostat system will be studied.

The chaotic motion is sensitive to the initial conditions. Trajectories with close initial conditions quickly become uncorrelated. In this section, two subsystems begin with two different initial conditions that will be synchronized by several methods.

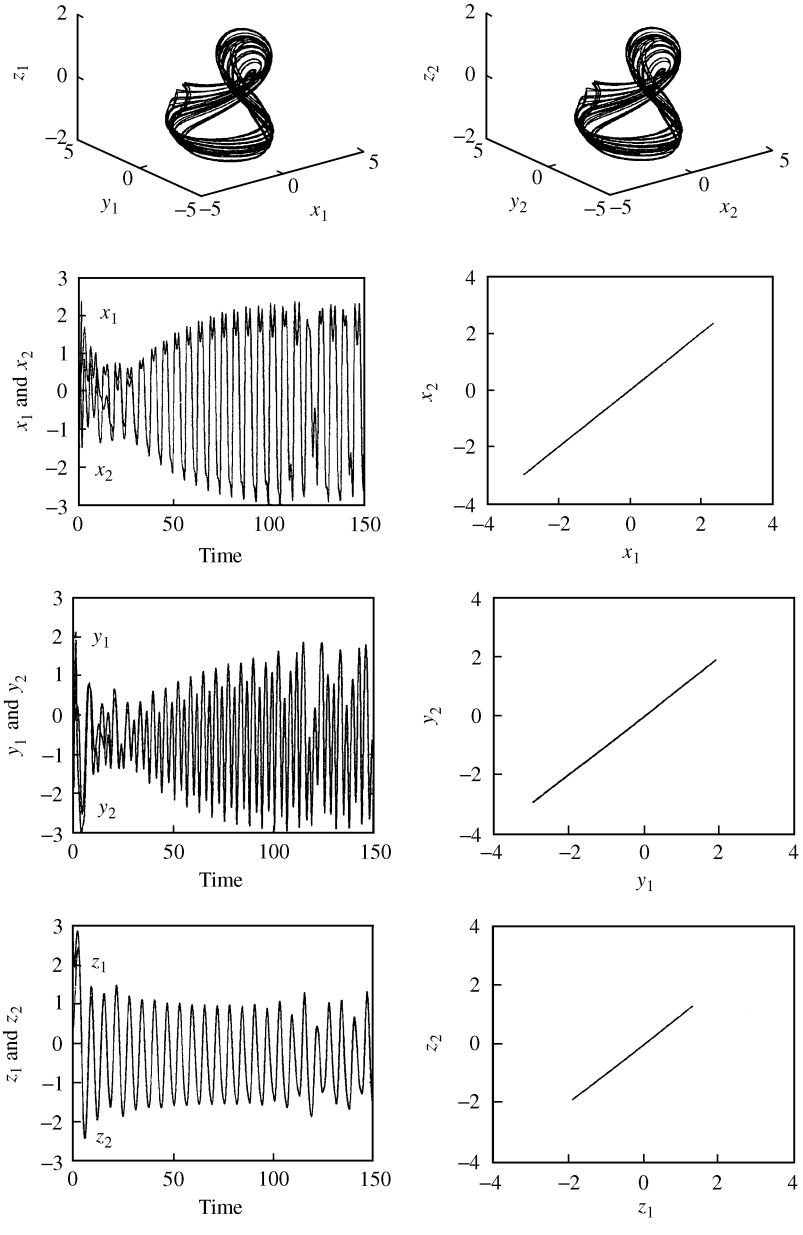

Figure 16. Phase portraits of both subsystems, time history of x_1 and x_2, y_1 and y_2, z_1 and z_2, x_1 versus x_2, y_1 versus y_2 and z_1 versus z_2. After 83 s, synchronization approached.

Equation (1) can be expressed as two subsystems

$$\dot{x}_1 = f_1(x_1, y_1, z_1), \qquad \dot{y}_1 = f_2(x_1, y_1, z_1), \qquad \dot{z}_1 = f_3(x_1, y_1, z_1), \tag{15}$$

$$\dot{x}_2 = f_1(x_2, y_2, z_2), \qquad \dot{y}_2 = f_2(x_2, y_2, z_2), \qquad \dot{z}_2 = f_3(x_2, y_2, z_2), \tag{16}$$

if $(x_1(0), y_1(0), z_1(0)) = (x_2(0), y_2(0), z_2(0))$, the phase portraits of equations (15) and (16) will be the same.

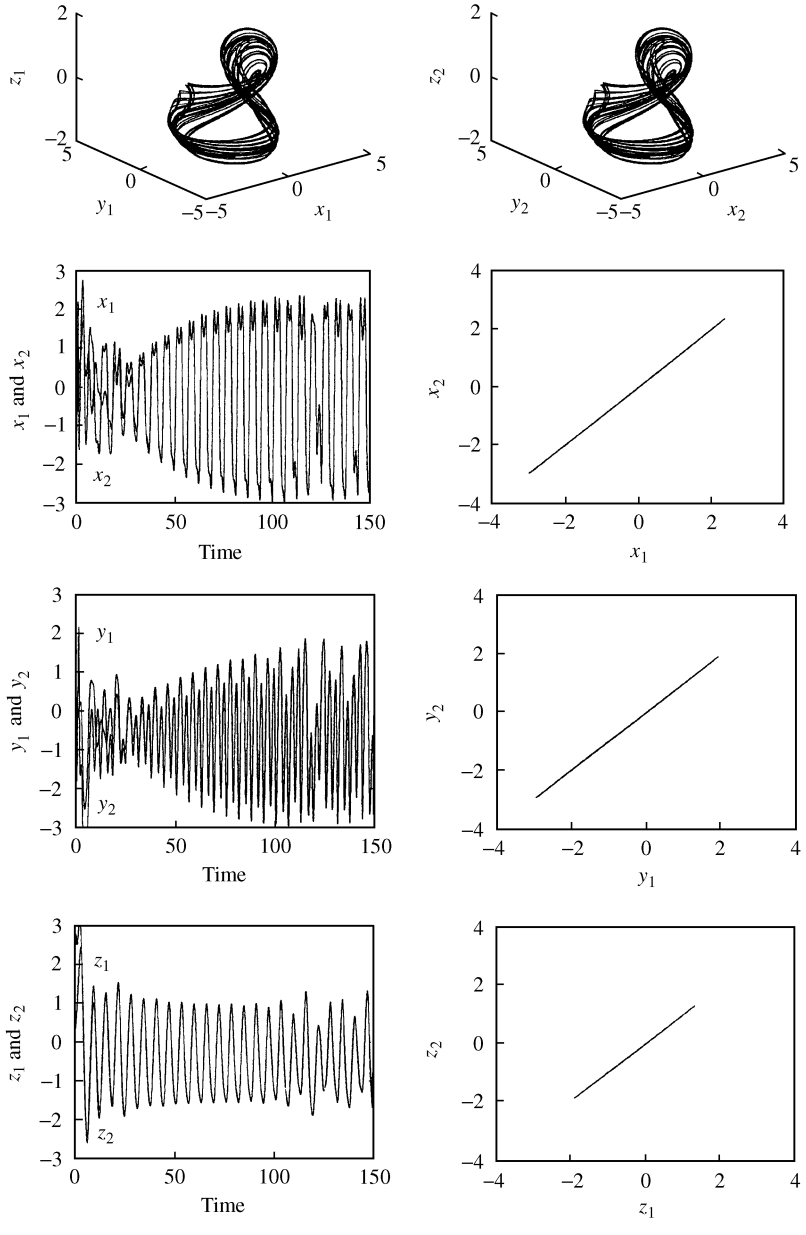

Figure 17. Phase portraits of both subsystems, time history of x_1 and x_2, y_1 and y_2, z_1 and z_2, x_1 versus x_2, y_1 versus y_2 and z_1 versus z_2. After 75 s, synchronization approached.

In section 6, the system has only one attractor that has been shown by the MICM method. This attractor can be obtained for the initial conditions $(x_1(0),\ y_1(0),\ z_1(0)) = (0{\cdot}1, 0{\cdot}2, 0{\cdot}3)$ and $(x_2(0),\ y_2(0),\ z_2(0)) = (1, 2, 3)$.

8.1. SYNCHRONIZATION BY ADDING LINEAR FEEDBACK TERM

In equation (16), the linear feedback term $\varepsilon(z_1 - z_2)$ is added in $f_3(x_2, y_2, z_2)$, then

$$\dot{x}_2 = f_1(x_2, y_2, z_2), \qquad \dot{y}_2 = f_2(x_2, y_2, z_2), \qquad \dot{z}_2 = f_3(x_2, y_2, z_2) + \varepsilon(z_1 - z_2) \tag{17}$$

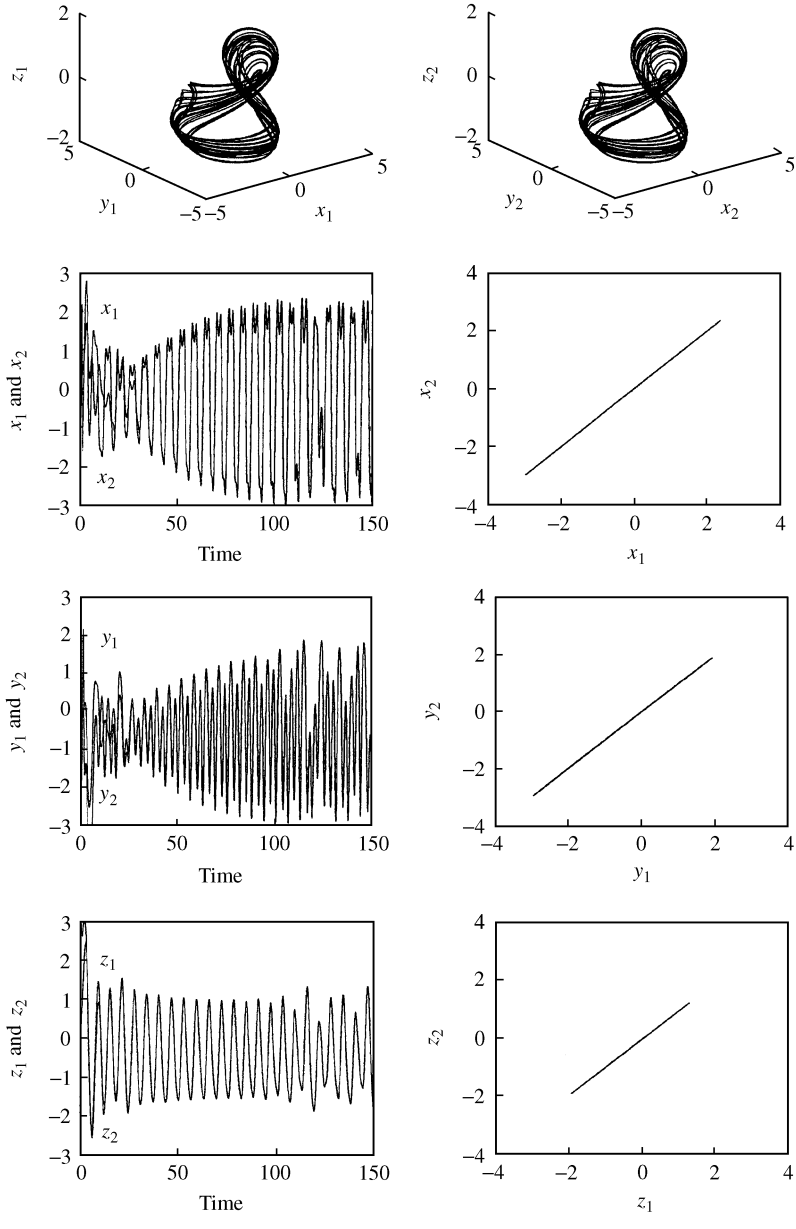

Figure 18. Phase portraits of both subsystems, time history of x_1 and x_2, y_1 and y_2, z_1 and z_2, x_1 versus x_2, y_1 versus y_2 and z_1 versus z_2. After 98 s, synchronization approached.

if $\varepsilon = 0{\cdot}7$, the phase portraits of equations (15) and (17) are synchronized and the results are shown in Figure 16. After 83 s, both trajectories are synchronized.

8.2. SYNCHRONIZATION BY ADDING SINUSOID FEEDBACK TERM

The sinusoid feedback term $\varepsilon \sin(z_1 - z_2)$ is added in $f_3(x_2, y_2, z_2)$ and equation (16) can be rewritten as

$$\dot{x}_2 = f_1(x_2, y_2, z_2), \qquad \dot{y}_2 = f_2(x_2, y_2, z_2), \qquad \dot{z}_2 = f_3(x_2, y_2, z_2) + \varepsilon \sin(z_1 - z_2) \quad (18)$$

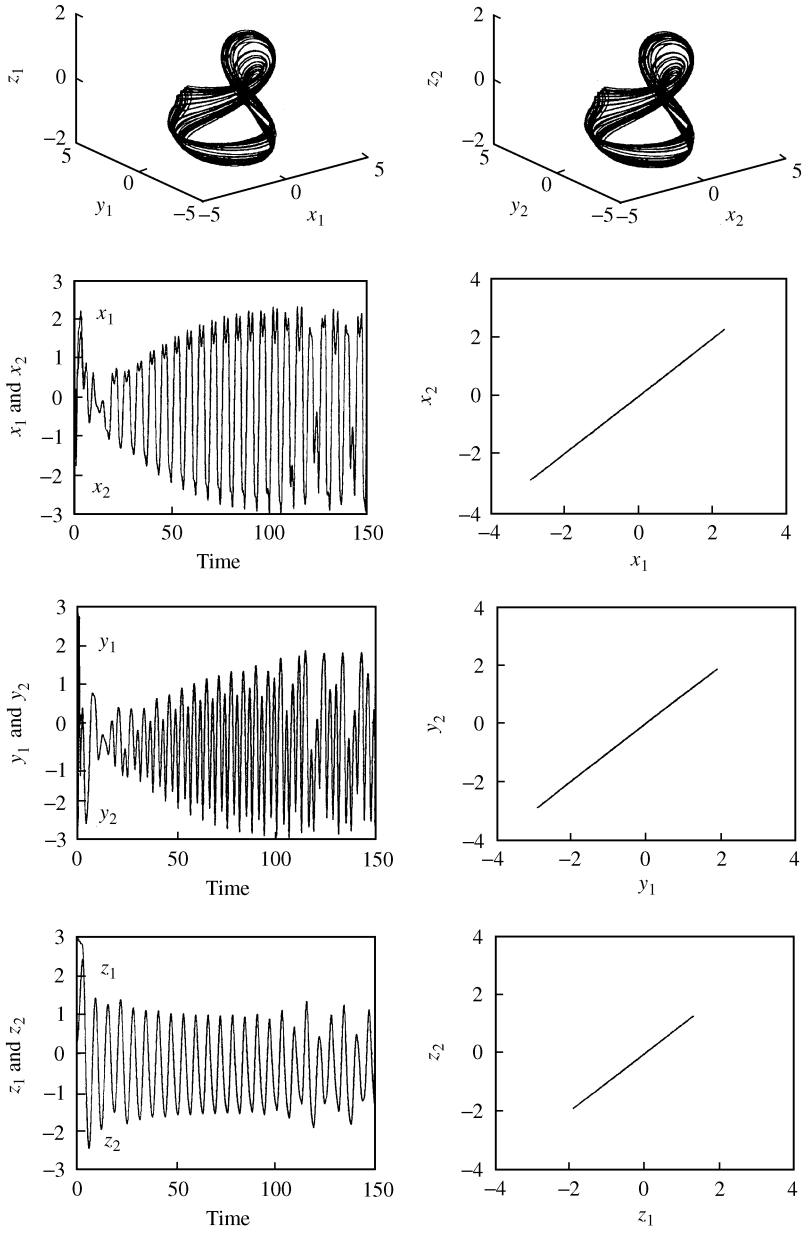

Figure 19. Phase portraits of both subsystems, time history of x_1 and x_2, y_1 and y_2, z_1 and z_2, x_1 versus x_2, y_1 versus y_2 and z_1 versus z_2. After 13·8 s, synchronization approached.

if $\varepsilon = 0{\cdot}7$, the phase portraits of equations (15) and (18) are synchronized and the results are shown in Figure 17. After 75 s, both trajectories are synchronized.

8.3. SYNCHRONIZATION BY ADDING EXPONENTIAL FEEDBACK TERM

The exponential feedback term $\varepsilon[\exp(z_1 - z_2) - 1]$ is added in $f_3(x_2, y_2, z_2)$, then equation (16) can be rewritten as

$$\dot{x}_2 = f_1(x_2, y_2, z_2), \quad \dot{y}_2 = f_2(x_2, y_2, z_2), \quad \dot{z}_2 = f_3(x_2, y_2, z_2) + \varepsilon[\exp(z_1 - z_2) - 1], \qquad (19)$$

if $\varepsilon = 0{\cdot}7$, the phase portraits of equations (15) and (19) are synchronized and the results are shown in Figure 18. After 98 s, both the trajectories are synchronized.

8.4. SYNCHRONIZATION BY COUPLED FORM OF THE SYSTEM

In equation (15), x_1^3, y_1^3, z_1^3 are replaced by $x_1x_2^2$, $y_1y_2^2$, $z_1z_2^2$ and in equation (16), x_2^3, y_2^3, z_2^3 are replaced by $x_2x_1^2$, $y_2y_1^2$, $z_2z_1^2$ respectively. Equations (15) and (16) can be rewritten as

$$\dot{x}_1 = f_1(x_1, y_1, z_1, x_2), \qquad \dot{y}_1 = f_2(x_1, y_1, z_1, y_2), \qquad \dot{z}_1 = f_3(x_1, y_1, z_1, z_2), \tag{20}$$

$$\dot{x}_2 = f_1(x_2, y_2, z_2, x_1), \qquad \dot{y}_2 = f_2(x_2, y_2, z_2, y_1), \qquad \dot{z}_2 = f_3(x_2, y_2, z_2, z_1). \tag{21}$$

In equation (21), linear feedback terms can be added in each function and expressed as

$$\dot{x}_2 = f_1(x_2, y_2, z_2, x_1) + \varepsilon(x_1 - x_2), \quad \dot{y}_2 = f_2(x_2, y_2, z_2, y_1) + \varepsilon(y_1 - y_2),$$

$$\dot{z}_2 = f_3(x_2, y_2, z_2, z_1) + \varepsilon(z_1 - z_2) \tag{22}$$

if $\varepsilon = 0{\cdot}7$, the phase portraits of equations (20) and (22) are synchronized and the results are shown in Figure 19. After 13·8 s, both the trajectories are synchronized.

The coupled form of the system method was synchronized more quickly than other methods at $\varepsilon = 0{\cdot}7$. Figure 20(a–d) shows the parameter ε versus synchronization time (ST). In Figure 21(a–d), when $\varepsilon \geqslant \varepsilon_0$, the transversal Lyapunov exponent (y_1) [21] is negative, and two chaotic oscillators can be completely synchronized. The parameter ε of the coupled form of the system method is the smallest when compared to other methods.

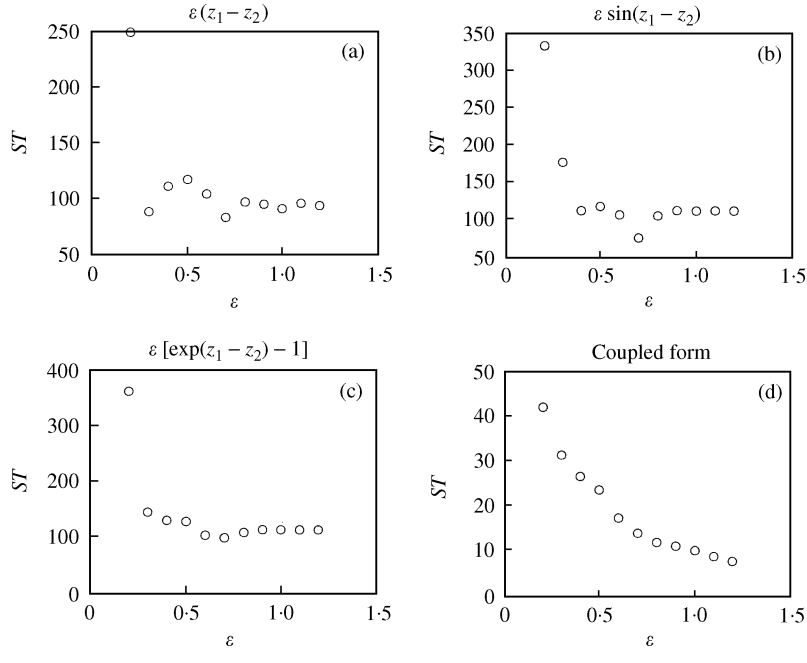

Figure 20. Synchronization time (ST) versus ε for: (a) adding linear feedback term; (b) adding sinusoid feedback term; (c) adding exponential feedback term; (d) coupled form of the system.

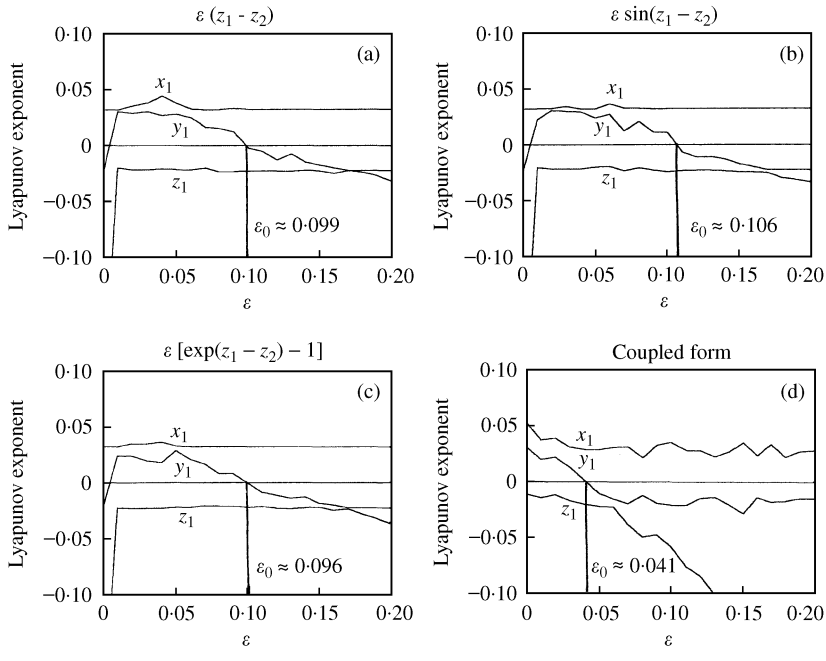

Figure 21. Transversal Lyapunov exponent (y_1) and ε_0 for: (a) adding linear feedback term; (b) adding sinusoid feedback term; (c) adding exponential feedback term; (d) coupled form of the system.

9. CONCLUSIONS

The dynamic system of the gyrostat system exhibits a rich variety of non-linear behaviors as certain parameters vary. Due to the effect of non-linearity, regular or chaotic motions may occur. In this paper, computational methods have been employed to study the dynamical behavior of the non-linear system.

The periodic and chaotic motion of the non-autonomous system are obtained by numerical methods such as power spectrum, period-T map, and Lyapunov exponents. Many non-linear and chaotic phenomena have been displayed in bifurcation diagrams. More information on the behavior of the periodic and the chaotic motion can be found in parametric diagrams. The changes of parameters play a major role in the non-linear system. Chaotic motion is the motion which has a sensitive dependence on initial conditions in deterministic physical systems. The chaotic motion has been detected by using Lyapunov exponents and Lyapunov dimensions. Although the results of the computer simulation have some errors, the conclusions match the bifurcation diagrams. Besides, the global analyses of the non-linear system have been obtained by using modified interpolated cell mapping (MICM).

The presence of chaotic behavior is generic for certain non-linearities, ranges of parameters and external force. Also, quenching of the chaos are presented so as to improve the performance of a dynamical system. The delayed feedback control, the addition of constant motor torque, the addition of periodic force, the addition of periodic impulse torque, injection of dither signal control, adaptive control algorithm, and bang–bang control are presented.

Synchronization of chaos has been presented by the addition of linear feedback terms, sinusoid feedback terms, exponential feedback terms and coupled form of the system methods. All control parameters ε are found.

ACKNOWLEDGMENTS

This research was supported by the National Science Council, Republic of China, under Grant Number NSC 89-2212-E-009-068.

REFERENCES

1. F. C. Moon 1992 *Chaotic and Fractal Dynamics*. New York: Wiley.
2. H. K. Khalil 1996 *Nonlinear System*, Englewood Cliffs, NJ: Prentice-Hall.
3. R. W. Brockett 1982 *Proceedings of the IEEE* 21*st Conference on Decision and Control*, 932–936. On conditions leading to chaos in feedback systems.
4. P. Holmes 1983 *Proceedings of the IEEE* 22*nd Conference on Decision and Control*, 365–370. Bifurcation and chaos in a simple feedback control system.
5. M. S. Nixon and A. K. Misra 1993 *Advances in the Astronautical Science* Part 1 **85**, 775–794. Nonlinear dynamics and chaos of two-body tethered satellite systems.
6. Zheng-Ming Ge 1999 *Nonlinear and Chaotic Dynamics of Satellites*. Taipei: Gau Lih Book Company.
7. Z.-M. Ge, C.-I. Lee, H.-H. Chen and S.-C. Lee 1999 *Journal of Sound and Vibration* 807–825. Nonlinear dynamics and chaos control of a damped satellite with partially-filled liquid.
8. C. D. Hall 1996 *Journal of Guidance*, *Control and Dynamics* **19**, Momentum transfer in two rotor gyrostats.
9. G. L. Gary, D. C. Kammer and I. Dobson 1992 *Advances in the Astronautical Sciences* Part 1 **79**, 593–612. Chaos is an attitude maneuver of a damped satellite due to time-periodic perturbations.
10. S. Paul Raj, S. Rajasekar and K. Murali 1999 *Physics Letters A* **264**, 283–288. Coexisting chaotic attractors, their basin of attractions and synchronization of chaos in two coupled duffing oscillators.
11. P. Frederickson, J. L. Kaplan, E. D. Yorke and J. A. Yorke 1983 *Journal of Differential Equations* **49**, 185–207. The Lyapunov dimension of strange attractors.
12. Z. M. Ge and S. C. Lee 1997 *Journal of Sound and Vibration*, **199**, 189–206. A modified interpolated cell mapping.
13. S. Sinha, R. Ramaswamy and J. S. Rao 1991 *Physica D* **43**, 118–128. Adaptive control in nonlinear dynamics.
14. Y. Braiman and I. Goldhirsh 1991 *Phyiscal Review Letters* **66**, 2545–2548. Taming chaotic dynamics with weak periodic perturbations.
15. E. Ott, C. Grebogi and J. A. Yorke 1990 *Physical Review Letters* **64,** 1196–1199. Controlling chaos.
16. B. A. Huberman and Lumer 1990 *IEEE Transaction on Circuits and Systems* **37**, 547–550. Dynamics of adaptive system.
17. C. C. Fuh and P. C. Tung 1997 *Physica Letters A* 228–234. Experimental and analytical study of diether signal in a class of chaotic system.
18. M. Lakshmanan and K. Murali 1996 *Chaos in Nonlinear Oscillators*: *Controlling and Synchronization*. Singapore: World Scientific.
19. G. Chen and X. Dong 1998 *From Chaos to Order*. Singapore: World Scientific.
20. T. Kapitaniak 1996 *Controlling Chaos*. London: Academic Press.
21. Hua-Wei Yin, Jian-Hua Dai and Hong-Jun Zhang *Physical Review E* **58**, 5683–5688. Phase effect of two coupled periodically driven Duffing oscillators.